Diamagnetic Raman Optical Activity

Deutsche Ausgabe: DOI: 10.1002/ange.201600058
Internationale Ausgabe: DOI: 10.1002/anie.201600058

Diamagnetic Raman Optical Activity of Chlorine, Bromine, and Iodine Gases

*Jaroslav Šebestík, Josef Kapitán, Ondřej Pačes, and Petr Bouř**

Abstract: *Magnetic Raman optical activity of gases provides unique information about their electric and magnetic properties. Magnetic Raman optical activity has recently been observed in a paramagnetic gas (Angew. Chem. Int. Ed.* ***2012****, 51, 11058; Angew. Chem.* ***2012****, 124, 11220). In diamagnetic molecules, it has been considered too weak to be measurable. However, in chlorine, bromine and iodine vapors, we could detect a significant signal as well. Zeeman splitting of electronic ground-state energy levels cannot rationalize the observed circular intensity difference (CID) values of about* 10^{-4}*. These are explicable by participation of paramagnetic excited electronic states. Then a simple model including one electronic excited state provides reasonable spectral intensities. The results suggest that this kind of scattering by diamagnetic molecules is a general event observable under resonance conditions. The phenomenon sheds new light on the role of excited states in the Raman scattering, and may be used to probe molecular geometry and electronic structure.*

Different interaction of molecules with left and right circularly polarized light (CPL) in the presence of magnetic field can be explored in optical devices and provides unique information about geometry and electronic structure of molecules. The Faraday effect, for example, is widely used in analytical chemistry, optical instrumentation, and laser and communication appliances.[1] Likewise, the magnetic circular dichroism spectroscopy matured into a useful tool to probe geometry and electronic states in a wide range of systems including new fullerene materials.[2] CPL components in the interstellar space, possibly caused by supernova magnetic fields,[3] have even been suggested to be responsible for the chirality encountered in living organisms.[4]

Recently, we reported observation of another phenomenon, paramagnetic Raman optical activity (ROA) of gas-phase NO_2.[5] The ROA spectrometer measures a tiny intensity difference in scattering of the right and left CPL ($I_R - I_L$). For the nitrogen dioxide the observation was possible due to the presence of a free electron lending it its magnetic moment of the order of the Bohr magneton (ca. 9.27×10^{-24} J T^{-1}). In addition, a near resonance of the incident laser light with NO_2 electronic states increased the Raman cross-section and made the observation easier. The effect was explained on the basis of ground-state rotational energy levels split in the external magnetic field, which also provided selection rules for the observed transitions. For example, absorption of left or right CPL can occur only when the magnetic quantum number changes by a unity.[6]

Such ground-state splitting would not allow for a similar detectable event in the diamagnetic gases, where the magnetic moment is close to the nuclear magneton (5.05×10^{-27} J T^{-1}), that is, 1840 times smaller than in the paramagnetic case. To our great surprise, however, the Cl_2, Br_2 and I_2 halogen gases or vapors, when kept in the magnetic field, exhibited a strong ROA signal as well. This can be explained by a different mechanism in diamagnetic molecules, taking into account interplay between the ground and excited electronic states and their rovibronic sub-levels. In particular, the excited electronic states are paramagnetic, split in the magnetic field much more than the ground state, and are thus largely responsible for the discrimination of the left and right CPL, even when the diamagnetic halogen species are involved (Figure 1).

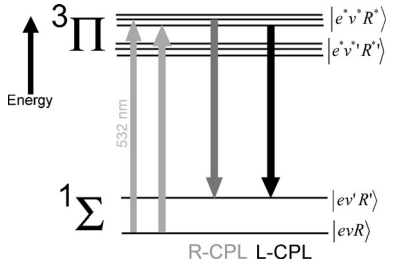

Figure 1. Simplified scheme of halogen energy levels in a static magnetic field. The field causes a negligible splitting of electronic ground-state rotational sublevels (e), but the excited electronic states (e^*) are paramagnetic and split significantly. This provides a measurable difference in scattering of the right and left circularly polarized light. In addition, the near resonance of the $e \rightarrow e^*$ transition with the 532 nm laser excitation increases the efficiency of Raman scattering.

The effect thus reminds magnetic ROA sometimes observed for condensed-state diamagnetic molecules.[7] For them, the effect was explained as a consequence of the Faraday A-type contribution to magnetic ROA, invoking degenerate paramagnetic excited resonant electronic and vibrational states.[6a,7b] For the gases investigated in the present study, there are the rotational sublevels that provide

[*] Dr. J. Šebestík, O. Pačes, Prof. P. Bouř
Biomolecular Spectroscopy
Institute of Organic Chemistry and Biochemistry
Flemingovo náměstí 2, 16610 Prague (Czech Republic)
E-mail: bour@uochb.cas.cz
Dr. J. Kapitán
Department of Optics, Palacký University
17. listopadu 12, 77146 Olomouc (Czech Republic)

Supporting information and ORCID(s) from the author(s) for this article are available on the WWW under http://dx.doi.org/10.1002/open.201600058.

the key sensitivity to the magnetic field and the selection rules.

The wealth of excited electronic and vibrational levels of the halogen molecules is well-documented in a number of earlier studies.[8] Vibrational states of the ground and excited electronic states are quite different, which together with the spin-orbit interaction[9] yield from modest (Cl_2) to very strong (Br_2, I_2) absorption across the visible spectral range. Owing to the nearly continuous excited-state energy levels,[10] the 532 nm laser employed in the ROA spectrometer can easily "find" a resonating transition, which tremendously increases the Raman cross section and makes it possible to detect the scattered light even from low-concentrated gases or vapors.

Maximum experimental circular intensity differences (ratios of the ROA and Raman signals, $CID = (I_R - I_L)/(I_R + I_L)$) for Cl_2, Br_2 and I_2 are measured as 1.13×10^{-4}, 3.90×10^{-4}, and 5.25×10^{-4}, respectively. For the scattered circular polarized (SCP) ROA experiment presented here the sample is irradiated by unpolarized light. Although the magnitudes are still somewhat smaller than for the paramagnetic NO_2 molecule (where CID ca. 2.8×10^{-3} at the same field of ca. 1.2 tesla)[5] they are comparable to those typically detected in naturally chiral molecules, either in the gas (methyloxirane, CID ca. 1×10^{-4})[11] or liquid phase.[12]

The diamagnetic Raman and ROA spectra are quite specific for individual halogens. Iodine (I_2) Raman and ROA experimental and simulated spectra are plotted in Figure 2. The element has only one stable isotope, ^{127}I, which contributes to the relative simplicity of the signal. The Raman and ROA experimental bands of the I–I stretching fundamental and overtone vibrations arise as the strongest ones amidst many fluorescence signals and a broad fluorescence background (the latter was subtracted from the spectrum shown). The fluorescence signal is very complex, depends on the excitations wavelength and other experimental conditions,[13] and can also be observed in the condensed phase.[14] We also observed its minor variations with temperature and pressure.

The fundamental vibrational transition ($0 \rightarrow 1$ with respect to the corresponding harmonic oscillator quantum numbers, at 213 cm^{-1}) is rather weak, both in Raman and ROA, and the spectra are dominated by the $0 \rightarrow 2$ overtone band at 425 cm^{-1}. More often, such overtones may be visible in vibrational spectra due to anharmonicities in the nuclear potential; these are, however, small for I_2 and cannot explain the observations.[15] In our case the large intensity of the overtone transitions is due to coupling of the initial and final vibrational states by a resonating state, through the Frank–Condon factors. Detectable peaks of variable intensities appear within the entire wavenumber range, up to the $0 \rightarrow 11$ transition at 2278 cm^{-1}. Hot bands ($1 \rightarrow 2$ etc.) were included in the simulated spectra as well; their contribution to the total intensities, however, is rather minor.

The florescence does not provide any measurable ROA intensities. Above 2000 cm^{-1} the ROA background noise in the experiment is greater due to the lower sensitivity of the coupled charge device (CCD) detector. However, the vibrational transitions can clearly be identified in the ROA spectrum. For all I–I stretching transitions, a relatively simple "$-+$" (if seen from left to right) conservative ROA

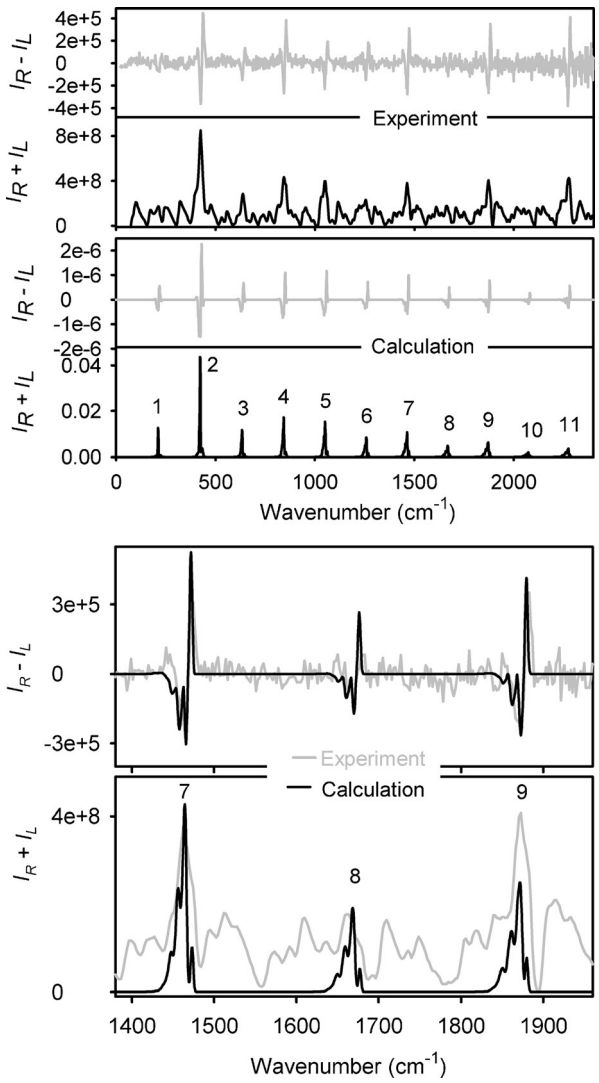

Figure 2. Experimental and simulated Raman ($I_R + I_L$) and ROA ($I_R - I_L$) spectra of iodine gas (I_2); vibrational quantum numbers for the $0 \rightarrow N$ transitions are indicated (top: whole spectrum, bottom: a detail). Computational units are arbitrary and only the ROA/Raman ratio can be compared to experiment.

signal appears, often accompanied by weaker bands, and the bands at higher wavenumbers are split more than at lower ones.

In the simulations the first $^3\Pi$ electronically excited state was modeled using experimentally determined parameters and analytical rotational wavefunctions (see the Methods Section and the Supporting Information). The theory reproduces the observations quite faithfully. For example, the high wavenumber splitting and asymmetry of the Raman and ROA bands are reproduced as well, which suggests that the approximate model based on one excited electronic state resonating with the 532 nm laser radiation is for the I_2 molecule reasonably realistic.

Bromine gas (Br_2) spectra are plotted in Figure 3. In this case the Raman bands are not affected by the fluorescence background as strongly as for I_2. The fundamental ($0 \rightarrow 1$) band at 319 cm^{-1} is the strongest one, and as for I_2 the

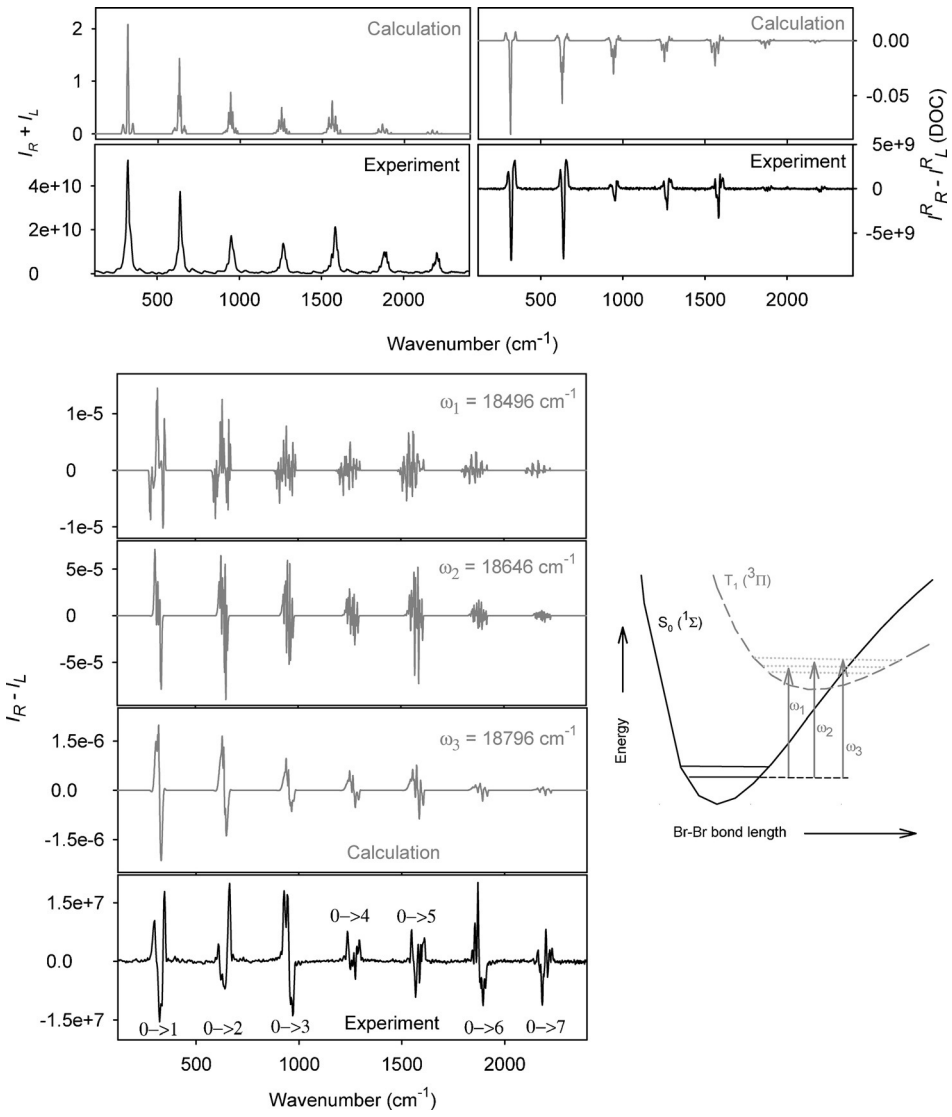

Figure 3. Experimental and simulated Raman ($I_R + I_L$), degree of circularity [$I^R{}_R - I^R{}_L$ (DOC)], and ROA ($I_R - I_L$) spectra of Br_2. The ROA simulations were performed for three excitation frequencies (ω_1, ω_2 and ω_3). As schematically depicted on the drawing, the frequencies sample rovibrational levels in the electronically excited state ($^3\Pi$) differently, which leads to different ROA patterns.

overtone bands are rather strong and visible up to the 0→7 band at 2189 cm^{-1}.

We found it useful to measure also the degree of circularity (DOC, Figure 3 right top), which as in ROA is the difference of scattered intensities for right- and left-CPL, but measured when the sample is irradiated by right-CPL. DOC is usually normalized to the total radiation in the same way as CID, that is, $(I^R{}_R - I^R{}_L)/(I^R{}_R + I^R{}_L)$, the upper index relates to the polarization of the incident radiation; in the figure only the $I^R{}_R - I^R{}_L$ part is plotted. More importantly, the DOC indicates how the molecule "remembers" the incident polarization.[16] In a recent study, for example, we used DOC to identify circularly polarized luminescence,[17] present also in the so called induced-resonance ROA (IRROA) of europium complexes.[18] For the luminescence, the DOC was small and identical to SCP ROA. On the contrary, the large magnitude of DOC Br_2 spectra and their agreement with the simulations indicate true vibrational Raman transitions.

The bromine ROA spectra (Figure 3, bottom-left) are more complex than those of I_2. Both fundamental (0→1) and the 0→2 overtone bands exhibit a w-shape signal, while the 0→3 transition gives a "+−" nearly conservative couplet. As for I_2, the higher-frequency bromine transitions tend to be broad and have multiple components. The ROA spectra complexity is partially due to the presence of three stable isotopic species in natural bromine, that is, $^{79}Br_2$, $^{79}Br^{81}Br$, and $^{81}Br_2$ occurring in 51.1:100:48.9 molar ratio. Different vibrational frequencies cause additional band splitting, especially for the higher-frequency vibrations. In the homonuclear molecules ($^{79}Br_2$ and $^{81}Br_2$) some molecular states are unavailable if compared to $^{79}Br^{81}Br$, because of the Pauli exclusion principle.[19] However, these factors were involved in the simulation and cannot explain the sign-flipping and other intensity variations of the ROA bands. We thus assume a participation of multiple rovibronic levels of the excited electronic state schematically indicated in the energy/bond length plot in the Figure. Indeed, modeling of the spectra with three excitation frequencies partially mimicking such situation results in qualitatively similar changes in ROA intensities. For example, the excitation frequency $\omega_3 = 18796$ cm^{-1} seems to correspond reasonably well to the resonance conditions of the 0→3 transition, providing the observed +− couplet, whereas giving almost opposite signal for 0→2 than seen experimentally.

In addition to this complexity, we found a significant dependence of the ROA Br_2 spectra on laser power (see Figure S1 in the Supporting Information). The overtone bands are particularly vulnerable, and ROA signs can be changed. Visualization of the sample cell by a thermo-camera revealed a significant (few Kelvin) temperature increase of the cell walls during the irradiation, presumably indicating much higher temperature of the vapor in the laser beam. A saturation of bromine energy levels was confirmed by a nonlinear Raman scattering intensity dependence on the laser power. Simulations performed at different temperatures

(Figure S2) led to smaller intensity changes, suggesting that non-equilibrium processes and energy transfer contribute more to the observed dependence. In general, the intensity variations may thus be attributed to varying populations of the rotational and vibrational bromine levels and their interplay with the excited resonance states. No time dependence of the spectra was observed.

The chlorine ROA and Raman spectra (Figure 4) were the most difficult to measure, due to the small Raman cross-section. Also, they exhibit only a few features. The second (0→2) and higher overtone Raman bands are weak and their ROA bands invisible (data not shown). Only the fundamental vibration 0→1 at 547 cm^{-1} with a small but reproducible ROA signal could be measured. The simulation faithfully reproduces the Raman rotational broadening, as well as the prevalent negative character of the ROA signal. As for bromine, three chlorine species are possible, $^{35}Cl_2$, $^{35}Cl^{37}Cl$ and $^{37}Cl_2$, in 1.56:1.00:0.15 molar ratio. However, individual isotopic contributions are not visible due to the limited resolution. The decreasing resonant character of Raman scattering in the $I_2 \approx Br_2 > Cl_2$ series is thus nicely documented in the ROA spectra; for Cl_2 the weak resonance leads to a weak signal (almost forbidden for overtone vibrations), and weak ROA (excited electronic levels with large magnetic moments are not sufficiently discriminated by the probing excitation radiation).

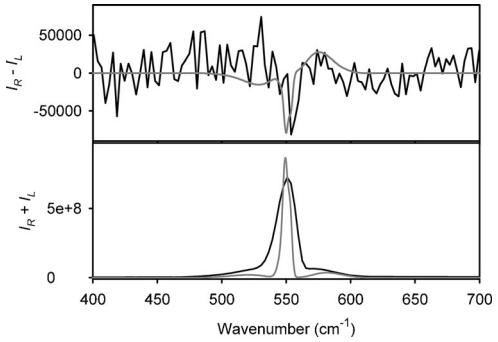

Figure 4. Experimental (black) and simulated (gray) ROA and Raman spectra of Cl_2 gas.

In conclusion, we measured the difference in scattering of the right and left circularly polarized light on diamagnetic Cl_2, Br_2, and I_2 molecules in the gas phase, which appeared to be a unique phenomenon enabled by the resonance of the impinging radiation with paramagnetic excited states, where rotational sublevels split in the static magnetic field. The simulations based on the free-rotator and single-resonating state approximations reasonably well reproduced the main features and trends in the experiments. The diamagnetic Raman optical activity thus promises to be a useful tool to probe electronic and vibrational molecular structure, may be potentially used for instrumental calibration, in optical components, and sheds more light on the physical origin of the two-photon Raman scattering.

Experimental Section

Raman and ROA spectra of Cl_2 gas and saturated Br_2 and I_2 vapors were obtained at 298 K and atmospheric pressure using the ChiralRAMAN-2X instrument based on the design of W. Hug and G. Hangartner,[16] operating with 532 nm laser light, 7 cm^{-1} resolution, and SCP backscattering configuration. For Cl_2, laser power at the sample was 800 mW and collection time about 12 hours for each magnet orientation. For Br_2 and I_2 about 10 mW and several minutes was sufficient. A new asymmetric design of the magnetic cell (Figure S3) provided about five-fold greater signal compared to our previous setup.[5] Raman and ROA intensities were calibrated with a NIST standard reference material (SRM 2242). The absolute intensities cannot be measured; experimental and simulated spectra are given in instrumental and atomic units, respectively, and only the CID = ROA/Raman ratio is comparable to the simulations and across various experiments.

The simulation was based on the Fermi golden rule, that is, transition probabilities for the right and left CPL[5,6] and the algebra of angular momentum and free rotator wavefunctions.[19a,20] Further details are given in the Supporting Information. For example, relative intensities of the left/right-CPL were obtained as given in Equation (1):

$$I_{L/R} \approx (2J+1)(2J'+1)\,|\langle v \mid v^*\rangle\langle v^* \mid v'\rangle cg_2 u|^2 \qquad (1)$$

where J and J' are the rotational quantum numbers of the ground and excited state, v and v' are corresponding vibrational quantum numbers, $\langle v \mid v^*\rangle$ and $\langle v^* \mid v'\rangle$ are the Frank–Condon factors, the asterisk (*) denotes the resonating excited state, and u contains transition electric dipole moment components, the energy f function, and magnetic quantum numbers. The transitions are thus enabled by overlaps of vibrational wavefunctions of the ground ($^1\Sigma$) and excited ($^3\Pi$) electronic states. The overlaps are typically large because of the significant differences in nuclear potentials.[8a,b,d] In the simulations, we normalized relative Raman intensities of vibrational transitions to experimental peak areas.

Acknowledgements

The present study was supported by the Grant Agency (grant numbers 13-03978S, 14-00431S, and 16-05935S) of the Czech Republic.

Keywords: angular momentum theory · diamagnetic molecules · excited electronic states · magnetic field · Raman optical activity

How to cite: *Angew. Chem. Int. Ed.* **2016**, *55*, 3504–3508
Angew. Chem. **2016**, *128*, 3565–3569

[1] a) R. Serber, *Phys. Rev.* **1932**, *41*, 489–506; b) M. Koch, X. Luo, W. Mürtz, *Appl. Phys. B* **1997**, *64*, 683–688; c) H. Ganser, W. Urban, J. M. Brown, *Mol. Phys.* **2003**, *101*, 545–550; d) S. Vandendriessche, S. Van Cleuvenbergen, P. Willot, G. Hennrich, M. Srebro, V. K. Valev, G. Koeckelberghs, K. Clays, J. Autschbach, T. Verbiest, *Chem. Mater.* **2013**, *25*, 1139–1143.

[2] a) V. Andrushchenko, D. Padula, E. Zhivotova, S. Yamamoto, P. Bouř, *Chirality* **2014**, *26*, 655–662; b) P. Štěpánek, M. Straka, V. Andrushchenko, P. Bouř, *J. Chem. Phys.* **2013**, *138*, 151103; c) P. Štěpánek, V. Andrushchenko, K. Ruud, P. Bouř, *J. Phys. Chem. A* **2012**, *116*, 778–783; d) M. Seth, T. Ziegler, in *Advances in Inorganic Chemistry*, *Vol. 62* (Eds.: R. VanEldik, J. Harley), Elsevier, San Diego, **2010**, pp. 41–109; e) C. N. Tam, B. Wang, T. A. Keiderling, W. G. Golden, *Chem. Phys. Lett.* **1992**, *198*,

123 – 127; f) D. J. Shieh, S. H. Lin, H. Eyring, *J. Phys. Chem.* **1972**, *76*, 1844 – 1848; g) C. Djerassi, G. Barth, R. Records, E. Bunnenberg, W. Voelter, *J. Am. Chem. Soc.* **1971**, *93*, 2545 – 2547; h) P. J. Stephens, *J. Chem. Phys.* **1970**, *52*, 3489 – 3516.
[3] R. Beck, R. Wielebinski, in *Planets, Stars and Stellar Systems*, *Vol. 5* (Eds.: T. Oswalt, I. S. McLean, H. E. Bond, L. M. French, P. Kalas, M. A. Barstow, G. Gilmore, W. C. Keel), Springer, Berlin, **2013**, pp. 13:11 – 66.
[4] C. Giri, F. Goesmann, C. Meinert, A. C. Evans, U. J. Meierhenrich, *Top. Curr. Chem.* **2012**, *333*, 41 – 82.
[5] J. Šebestík, P. Bouř, *Angew. Chem. Int. Ed.* **2014**, *53*, 9236 – 9239; *Angew. Chem.* **2014**, *126*, 9390 – 9393.
[6] a) L. D. Barron, *Molecular Light Scattering and Optical Activity*, Cambridge University Press, Cambridge, **2004**; b) D. P. Craig, T. Thirunamachandran, *Molecular quantum electrodynamics*, Dover Publications, New York, **1998**; c) B. Wang, P. Bouř, T. A. Keiderling, *Phys. Chem. Chem. Phys.* **2012**, *14*, 9586 – 9593.
[7] a) L. D. Barron, *Nature* **1975**, *257*, 372 – 374; b) L. D. Barron, C. Meehan, J. Vrbancich, *J. Raman Spectrosc.* **1982**, *12*, 251 – 261.
[8] a) S. D. Peyerimhoff, R. J. Buenker, *Chem. Phys.* **1981**, *57*, 279 – 296; b) P. Baierl, W. Kiefer, *J. Raman Spectrosc.* **1975**, *3*, 353 – 369; c) S. Gerstenkorn, P. Luc, A. Raynal, J. Sinzelle, *J. Phys. (Paris)* **1987**, *48*, 1685 – 1696; d) A. Scaria, V. Namboodiri, J. Konradi, A. Materny, *J. Chem. Phys.* **2007**, *127*, 144305.
[9] M. I. Bernal-Uruchurtu, G. Kerenskaya, K. C. Janda, *Int. Rev. Phys. Chem.* **2009**, *28*, 223 – 265.
[10] P. Baierl, W. Kiefer, *J. Raman Spectrosc.* **1981**, *11*, 393 – 405.
[11] J. Šebestík, P. Bouř, *J. Phys. Chem. Lett.* **2011**, *2*, 498 – 502.
[12] L. Nafie, *Vibrational optical activity: Principles and applications*, Wiley, Chichester, **2011**.
[13] W. F. Howard, L. Andrews, *J. Raman Spectrosc.* **1974**, *2*, 447 – 462.
[14] W. Kiefer, H. J. Bernstein, *J. Raman Spectrosc.* **1973**, *1*, 417 – 431.
[15] W. Guo, D. Wang, J. S. Hu, Z. K. Tang, S. Du, *Appl. Phys. Lett.* **2011**, *98*, 043105.
[16] W. Hug, G. Hangartner, *J. Raman Spectrosc.* **1999**, *30*, 841 – 852.
[17] T. Wu, J. Kapitán, V. MaŠek, P. Bouř, *Angew. Chem. Int. Ed.* **2015**, *54*, 14933 – 14936; *Angew. Chem.* **2015**, *127*, 15146 – 15149.
[18] S. Yamamoto, P. Bouř, *Angew. Chem. Int. Ed.* **2012**, *51*, 11058 – 11061; *Angew. Chem.* **2012**, *124*, 11220 – 11223.
[19] a) P. R. Bunker, P. Jensen, *Molecular Symmetry and Spectroscopy*, NCR Research Press, Ottawa, **2006**; b) G. Herzberg, *Molecular Spectra and Molecular Structure*, D. Van Nostrand Company Inc., Princeton, New Jersey, **1945**.
[20] R. N. Zare, *Angular Momentum*, Wiley, New York, **1988**.
[21] G. Herzberg, *Constants of Diatomic Molecules*, Van Nostrand-Reinhold, New York, **1979**.
[22] R. Luypaert, J. Van Craen, J. Coremans, G. De Vliegert, *J. Phys. B* **1981**, *14*, 2575 – 2584.
[23] S. Gerstenkorn, P. Luc, *J. Phys. (Paris)* **1989**, *50*, 1417 – 1432.
[24] a) R. F. Barrow, K. K. Yee, *J. Chem. Soc. Faraday Trans. 2* **1973**, *69*, 684 – 800; b) M. Broyer, J. C. Lehmann, J. Vigue, *J. Phys. (Paris)* **1975**, *36*, 235 – 241; c) J. L. Steinfeld, R. N. Zare, L. Jones, M. Lesk, W. Klemperer, *J. Chem. Phys.* **1965**, *42*, 25 – 33.
[25] W. M. M. Haynes, D. R. Lide, *CRC Handbook of Chemistry and Physics*, *91st ed.*, NIST, Internet Version 2011, **2011**.

Received: January 4, 2016
Published online: February 4, 2016

